Lawrence Berkeley National Laboratory

To be presented at the ASME Winter Annual Meeting, Technical Session on Heat Transfer in Nuclear Waste Disposal, Chicago, IL, November 16-21, 1980

LBL-10876

CONF-801102--17

HEAT TRANSFER IN UNDERGROUND HEATING EXPERIMENTS IN GRANITE, STRIPA, SWEDEN

Tin Chan, Iraj Javandel and Paul A. Witherspoon

April 1980

Prepared for the U.S. Department of Energy
under Contract W-7405-ENG-48

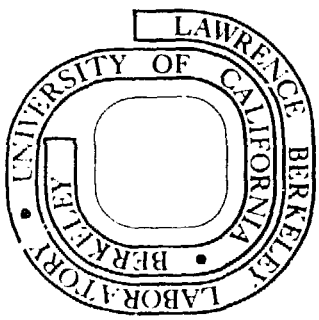

Submitted to:
Technical Session on Heat Transfer in Nuclear Waste Disposal
ASME Winter Annual Meeting,
Chicago, Illinois, November 16-21, 1980

LBL-10876

HEAT TRANSFER IN UNDERGROUND HEATING EXPERIMENTS IN GRANITE, STRIPA, SWEDEN

Tin Chan, Earth Sciences Division, Lawrence Berkeley Laboratory
Berkeley, California 94720

Iraj Javandel, School of Engineering, Shiraz University,
Shiraz, Iran

Paul A. Witherspoon, Earth Sciences Division, Lawrence Berkeley
Laboratory, Berkeley, California 94720

ABSTRACT

Electrical heater experiments have been conducted underground in granite at Stripa, Sweden, to investigate the effects of heating associated with nuclear waste storage. Temperature data from these experiments are compared with closed-form and finite-element solutions. Good agreement is found between measured temperatures and both types of models, but especially for a nonlinear finite-element heat conduction model incorporating convective boundary conditions, measured nonuniform initial rock temperature distribution, and temperature-dependent thermal conductivity. In situ thermal properties, determined by least-squares regression, are very close to laboratory values. A limited amount of sensitivity analysis is undertaken.

LIST OF SYMBOLS

Roman

a	radius of cylindrical or disc heat source (m)
b	half-length of heater (m)
c	specific heat (of solid) at constant pressure (J/kg-°C)
c_f	specific heat of water at constant pressure
erf	error function
FEM	finite-element model
g	gravitational acceleration (m/s^2)
h	heat transfer coefficient (W/m^2-°C)
I_o	modified Bessel function of first kind, zeroth order
k	thermal conductivity (W/m-°C)
k^{in}	intrinsic permeability (m^2)
ℓ	characteristic length of system (m)
q_ℓ	heat generation rate per unit length of line heater (W/m)
q_c	heat generation rate per unit volume of cylindrical heater (W/m^3)
q_d	heat generation rate per unit area of disc heater (W/m^2)
r	radial coordinate in cylindrical system (m)
r'	integration variable (m)
Ra	dimensionless Rayleigh number
t	time (s or day)
T	temperature (°C)
ΔT	temperature rise (°C)
z	axial coordinate in cylindrical system (m)

Greek

α_f	volumetric thermal expansion coefficient of water (m^3/m^3-°C)
κ	thermal diffusivity (m^2/s)
μ	integration variable (s)
μ_f	dynamic viscosity of water (kg/m-s)
ρ	density (kg/m^3)
ρ_f	density of water (kg/m^3)

INTRODUCTION

In order to investigate the heat transfer and related processes in an underground environment similar to that expected in a mined nuclear waste repository in hard rock, a series of in situ heating experiments were conducted at a depth of approximately 338 m in a granite body adjacent to an abandoned iron ore mine at Stripa, Sweden. These experiments are part of a Swedish-United States cooperative program to study radioactive waste storage [1,2].

The purpose of this paper is to compare, in some detail, the temperatures measured in one of the heater experiments with the results of both closed-form and finite-element solutions. This comparison will lead to a better understanding of the heat transfer processes associated with underground nuclear waste storage in granite. Results for thermally induced displacements and stresses have been presented elsewhere [2,4].

The finite element thermal analyses to be discussed took into account (a) forced convective boundary conditions at the surfaces of the mine drifts resulting from ventilation, (b) nonuniform initial rock temperatures, (c) material nonlinearity, and (d) other details of operating conditions. A limited amount of sensitivity analysis has been undertaken to study the influence of various parameters on the thermal field.

THE HEATER EXPERIMENTS

There were three heater experiments. Two "full-scale" experiments simulated the short-term near-field heating effects of an individual nuclear waste canister at two different thermal power levels. The third experiment used an array of scaled-down heaters with decaying power to study the thermal interac-

tion between adjacent nuclear waste canisters in a repository over an equivalent period of approximately a decade. In the time-scaled experiment, the law of similitude for linear heat conduction was utilized to accelerate the time evolution by a factor of 10.2 by reducing the power and linear dimensions of the heaters and their spacing by a factor of 3.2.

A vertical section is shown in Fig. 1 for one of the full-scale heater experiments. In the full-scale experiments, electrical heater canisters, 0.32 m in diameter and 2.6 m in height, were placed in vertical 0.406 m diameter drill holes so that the midplane is 4.25 m below the floor of the heater drift. The two main heaters were operated at constant powers of 3.6 kW and 5 kW, respectively, corresponding to the initial thermal output of a canister of reprocessed high-level waste from light-water reactors approximately 5 and 3.5 years out of the reactor [3].

Discussion in this paper will focus mainly on the thermal field for the 3.6 kW full-scale experiment.

CLOSED-FORM SOLUTIONS

Assumptions and Approximations

Prior to conducting the experiments preliminary calculations were made to predict the expected rock temperatures around the heaters [6]. To simplify the calculations the problem was idealized using the following assumptions:

(a) conduction is the only mode of heat transfer;

(b) the rock medium is continuous, isotropic, and homogeneous;

(c) the rock medium is either infinite or semi-infinite. In the latter case it was assumed that the rock is bounded above by an imaginary plane coinciding with the floor of the heater drift.

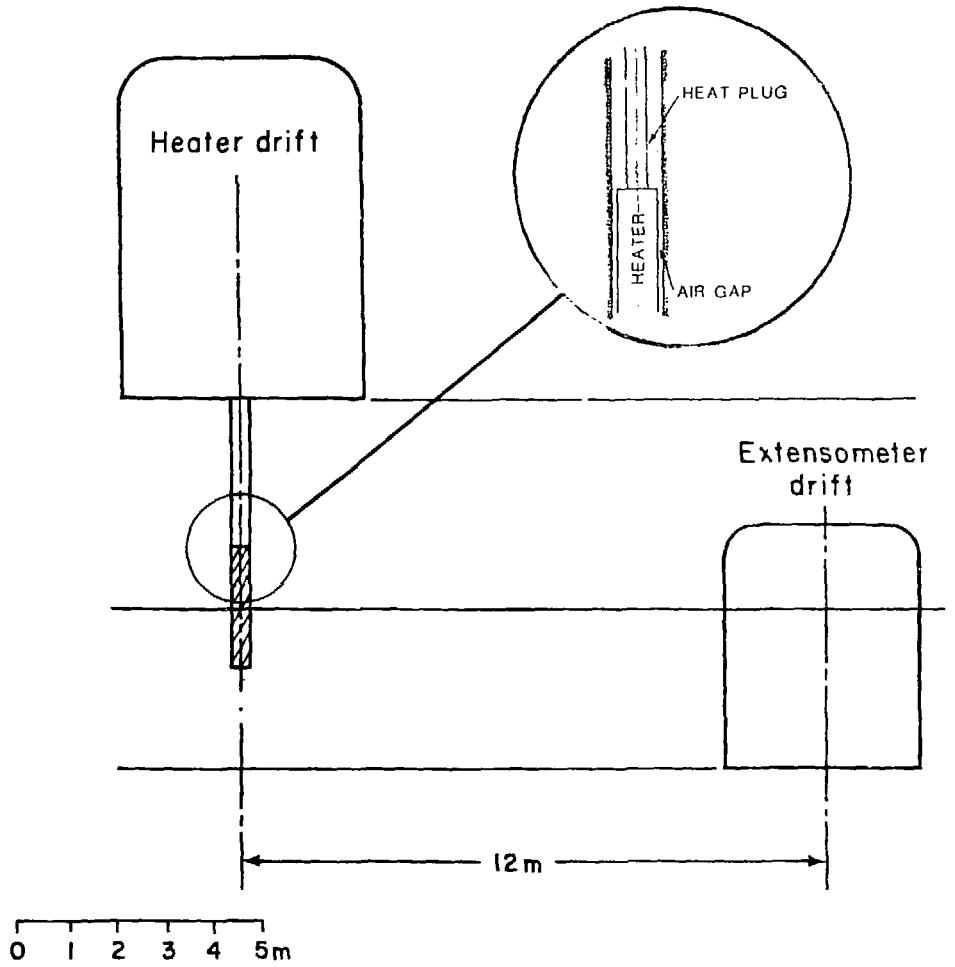

Fig. 1. Geometry of the 3.6 kW heater experiment, vertical section.

(d) the heaters are in perfect thermal contact with the rock;

(e) before the heaters are turned on the initial rock temperature is uniform;

(f) both the heaters and the rock have the same constant (temperature-independent) thermal properties.

In general, heat transfer in a rock mass may involve both conduction and groundwater convection. If the granite rock mass at Stripa is treated as a porous medium, the Rayleigh number, the ratio of heat transfer due to natural convection to that due to conduction [8], can be shown (Appendix A) to be very small because of the low permeability. It is, therefore, a good first approximation to neglect convection.

Closed-form integral solutions to the idealized linear thermal conduction problem have been obtained using the Green's function method [6,7]. Solutions for a time-varying, finite-length line heat source, a finite-length cylindrical heat source, and a disc source are given in Appendix B. The integrals were evaluated numerically using the Romberg quadrature. Isothermal boundary condition at the floor of the heater drift is simulated by image heat sinks.

Numerical comparison of rock temperatures due to a line heat source and a cylindrical heat source has demonstrated that, except at very short times (less than a day), the two types of heat sources give rise to practically identical rock temperatures.

Thermal properties (Table 1) determined using small intact specimens of Stripa granite [9] were used in these calculations. Density and specific heat were found to be practically independent of temperature over the range of rock temperatures expected in the heater experiments. The thermal conductivity was found to decrease with temperature at the rate of approximately 1% per 10°C temperature rise:

$$k(T) = 3,60 - 0.37 \times 10^{-2}T \quad W/m\text{-}°C \qquad (1)$$

The value, 3.2 W/m-°C, corresponding to an average rock temperature of 100°C, was used in the calculations.

Table 1. Thermal Properties

Property	Symbol	Value: Stripa granite	Value: Vermiculite (heat plug)	Unit
thermal conductivity	k	3.2*	0.063	W/m-°C
specific heat	c	837	921	J/kg-°C
density	ρ	2600	92.9	kg/m^3
diffusivity	$\kappa = k/\rho c$	1.47×10^{-6}	7.36×10^{-7}	m^2/s

* Value at approximately 100°C. See Eq. (1) for temperature dependence.

General Comparison with Field Data

In Fig. 2, the actual thermocouple readings in the midplane of the 3.6 kW full-scale experiment are overlaid on the isotherms calculated using the closed-form solution with isothermal boundary condition. The general agreement indicates that conduction is the predominant heat transfer mechanism. Apparently, there is no significant anisotropy in the thermal properties of the rock. Furthermore, it can be inferred from the agreement between measured and calculated temperatures for the time-scaled experiment (see [8] for typical results), the design of which was based on linear conduction, that the temperature dependence of the thermal conductivity does not appear to lead to severe nonlinearity.

In Fig. 3, calculated and measured rock temperatures at several thermocouples located at various elevations in the vertical hole nearest to the

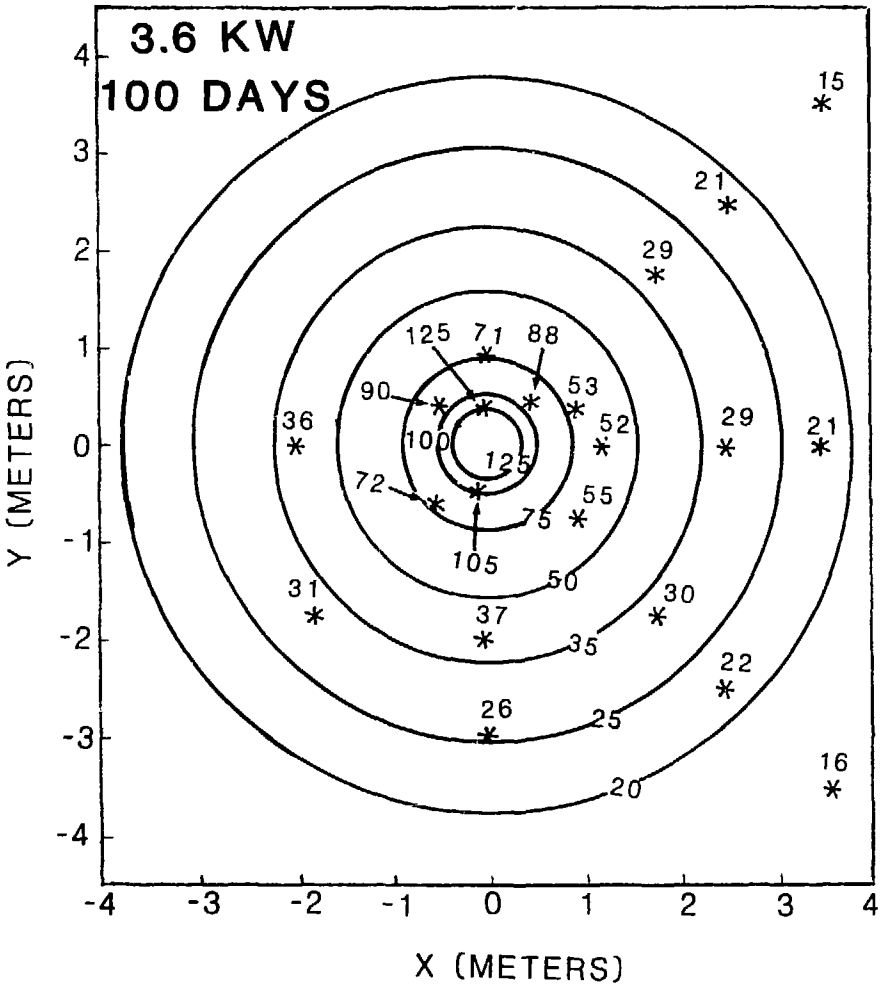

Fig. 2. Horizontal section through midplane of the 3.6 kW heater (at center) showing calculated isotherms (closed-form solution) together with measured temperatures at various thermocouple locations (asterisk) after 100 days. (XBL 804-9274)

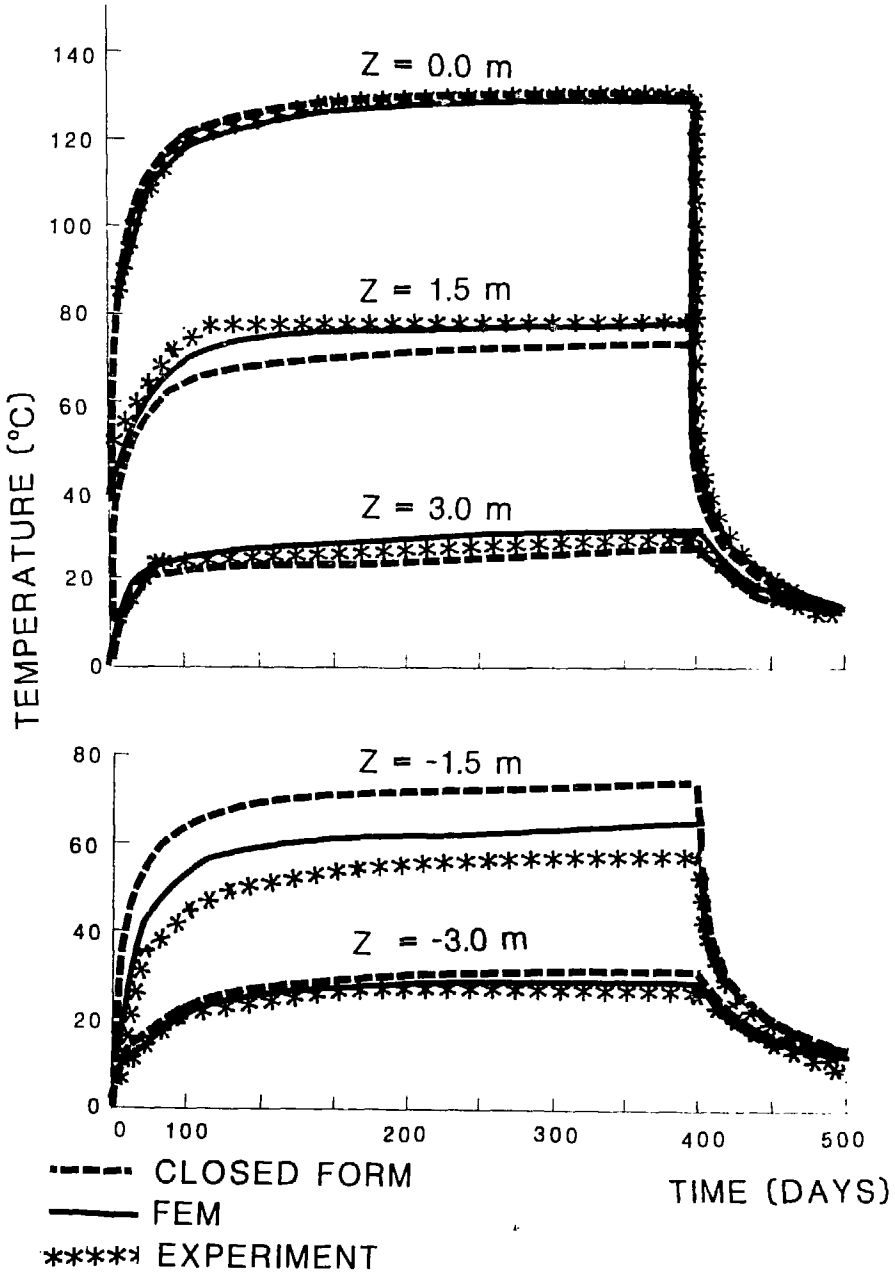

Fig. 3. Measured and calculated temperatures as a function of time at radial distance 0.4 m from the axis of the 3.6 kW heater and at various elevations. (XBL 804-9273)

3.6 kW heater (at 0.4 m radius)* have been plotted as a function of time. Evidently, there is little change in the thermal properties of the rock during the cooling period, i.e., after the heater has been turned off at 398 days. Detailed discussion of this figure will be given in the next section.

In situ Thermal Properties

In situ thermal properties have been extracted statistically from the first 70 days of temperature data for the 5 kW experiment by means of least-squares fit to the closed-form solution [11]. Only low-temperature data were used for this purpose because many of the high-temperature thermocouples had been corroded. At an average rock temperature of 23°C the in situ thermal conductivity was found to be 3.69 W/m°C, approximately 5% higher than the laboratory value at the same temperature, while the thermal diffusivity was 1.84 $\cdot 0^{-6}$ m^2/s, 13% higher than the corresponding laboratory value. If the density and specific heat were held fixed, then the best-fit thermal conductivity was 3.55 W/m-°C, only 1% higher than the laboratory value. However, the "goodness of fit" was better for the two-parameter fit than for the one-parameter fit. The slightly higher in situ thermal conductivity and diffusivity may be due to the presence of groundwater in the rock mass in contrast to the dry specimens used for laboratory testing. The remarkable thing, however, is not their difference but rather the lack of significant difference in spite of the presence of discontinuities in the rock mass. This is in sharp contrast to the dramatic "size effect" on the mechanical properties of rock reported by a number of authors (see [12] for a review).

* Throughout this paper positions will be specified in a local cylindrical coordinate system with the axis of the full-scale heater as the z-axis. The plane z = 0 is the planned (horizontal) midplane of the heater. Above this plane, z > 0.

Discrepancies

Although there is general agreement between theory and experiment, closer examination of comparison plots such as Fig. 3 has revealed that (a) above the planned horizontal heater midplane (z = 0 plane), measured rock temperatures are higher than predicted by the isothermal boundary condition model (dashed line in Fig. 3), whereas below the midplane, measured temperatures are lower than predicted, and (b) rock temperatures measured above the horizontal midplane are higher than those at equal distances below the midplane. These trends generally hold for all three heater experiments. For the 3.6 kW experiment the asymmetry in the measured temperatures about the horizontal midplane and the discrepancies between theory and field data are most serious for thermocouples at r = 0.4 m and z = $\pm$ 1.5 m. With increasing radial and vertical distances from the heater, the discrepancies diminish.

A number of possible causes may be suggested for the discrepancies noted above, including: (a) groundwater/steam convection in the rock; (b) steam forming in the heater hole, convecting upward in the air gap between the heater canister and the wall of the hole, and recondensing in the vermiculite heat plug (see inset of Fig. 1); (c) errors in positions of the heater or the thermocouples; (d) forced convection boundary conditions at the surface of the heater drift and extensometer drift; (e) heat loss through insufficient insulation at the heat plug so that natural convection is set up in the heater hole between the top of the heat plug and the floor of the heater drift; (f) nonuniform temperature distribution in the rock before the heaters were turned on; (g) temperature dependence of thermal properties of the rock; and (h) different thermal properties of the rock above and below the midplane

because of different degrees of water saturation and, possibly, damage to rock just below the floor of the heater drift during excavation.

Position of Heater

If groundwater convection or steam formation were responsible for the higher rock temperatures above the planned midplane, the vertical asymmetry would be expected to be more pronounced for the 5 kW experiment than for the 3.6 kW experiment because of the higher temperatures and thermal gradients in the former. Comparison of the field data for these two experiments shows that the opposite is true. This has led to the suspicion that the position of the 3.6 kW heater might be in error.

When the position was remeasured, it was found that the 3.6 kW heater was indeed installed 10-13 cm above the planned position. Some uncertainty in the exact position remains because of the irregular relief of the floor of the heater drift. Shifting the heater position up by 10 cm increases the calculated temperature at z = 1.5 m, r = 0.4 m by almost 7°C and decreases the temperature at z = 1.5 m, r = 0.4 m by 6°C at 100 days. Temperatures at these locations, which are close to the ends of the heater, are especially sensitive to the position of the heater. Temperatures at z = 0 are hardly effected by this shift at all. Thus more than 50% of the discrepancies between observed temperatures and the original close-form solution (Fig. 3) is removed by correcting for the vertical position of the heater.

FINITE ELEMENT MODEL

To assess the influence of the factors (d) - (h) listed in the last section, nonlinear thermal analyses were carried out using the finite-element

heat transfer code DOT [13]. The model used is an axisymmetric model with the axis of the heater as the axis of symmetry. The outside boundaries, at r = 100 m or z = ±100 m, are assumed insulated. Forced convection boundary conditions (with heat transfer coefficient, h = 3 W/m^2-°C, unless otherwise stated) are applied at the surfaces of the heater drift and extensometer drift to simulate mine ventilation. Further details of the model are discussed below for the 3.6 kW experiment.

Convection in Heater and Extensometer Drifts

Two sets of calculations were undertaken using the heater coefficients h = 3 W/m^2-°C and h = 8 W/m^2-°C, corresponding to air velocities of 1.1 m/s and 3.9 m/s, respectively, according to a standard formula for forced convective heat transfer [14]. Air temperature was taken to be 18°C in the heater drift and 10°C in the extensometer drift, probably within 2°C of the actual air temperature for the duration of the experiments.

The heater drift exerts a greater influence on the rock temperature than the extensometer drift. Maximum effect is felt by the rock at the floor of the heater drift. Before the heaters were turned on, the rock temperature there was 14°C. For h = 3 W/m^2-°C the calculated temperature at a represented point at the floor (r = 1.3 m, z = 4.25 m) rises to 18.2°C in 40 days, 19.7°C in 100 days, 20.8°C in 200 days, and 22.0°C in 380 days. Note that for the first 40 days or so heat is flowing from the warmer air into the cooler rock. In comparison with the closed-form isothermal boundary model, the model with heat transfer coefficient h = 3 W/m^2-°C predicts generally higher rock temperatures. Maximum difference is 8°C at z = 4.25 m (floor of drift), 4-5°C at z = 3 m, 3-4°C at z = 1.5 m, 1-2°C at z = 0, 1°C at z = -1.5 m, and less

than 1°C further into the rock. Although the effect of the convective boundary is small, it is in the right direction.

For h = 8 W/m^2-°C, maximum rock temperature at r = 1.3 m, z = 4.25 m (at the floor of the heater drift) is predicted to be 18.9°C. Temperatures at thermocouple locations are lower than for the case of h = 3 W/m^2-°C by 2°C (r = 0.4 m, z = 3 m) or less. Except at the drift floor where, unfortunately, the temperature has not been monitored, the differences between the temperatures calculated using the two different values of h are probably comparable to the uncertainties in the measurement. Consequently, it is not possible to use the field data to back-calculate the actual heat transfer coefficient. A limited amount of relevant temperature data for the 5 kW experiment seems to indicate a heat transfer coefficient closer to 8 W/m^2-°C.

For either value of h, the maximum rate of heat loss from the rock at the floor of the heater drift into the ventilation air is approximately 200 W.

Magnitudes of rock temperatures are affected only slightly (by less than 1°C) by forced convection ventilation in the extensometer drift. However, the lower air temperature in this drift (approximately 10°C compared with 18°C in the heater drift) has a very interesting effect on the temperature history, as illustrated in the semilog plot in Fig. 4. The original motivation for such a plot was to utilize the analogy between heat conduction and fluid flow in porous media to search for possible evidence of effects of discontinuities on the thermal properties of the rock mass. It is customary for groundwater hydrologists to employ this type of semilog plot to infer the transmissivity of an aquifer. In the simplest case the transmissivity is inversely proportional to the slope of the curve. Note that in Fig. 4 the scale was deliberately chosen

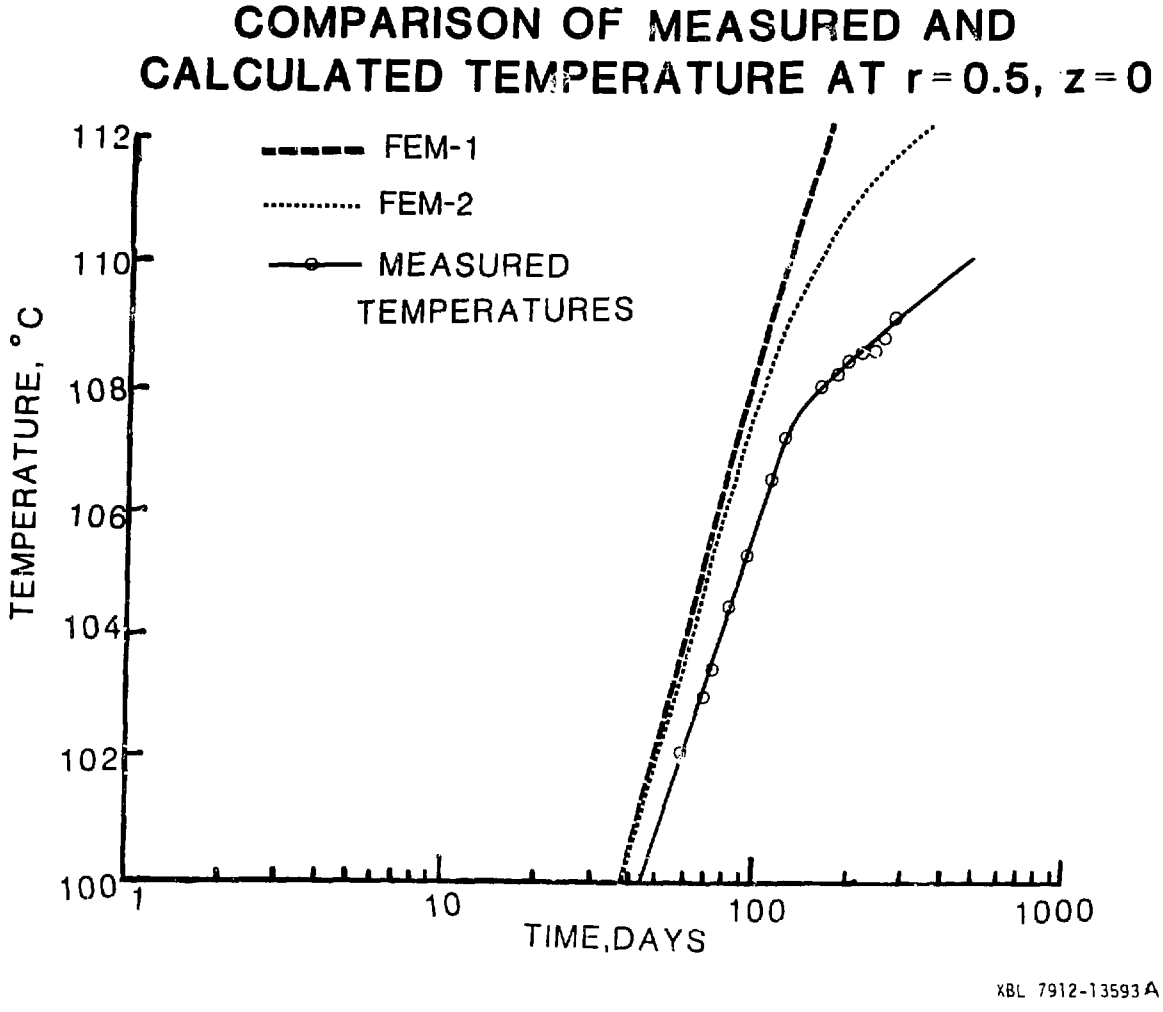

Fig. 4. Semilog plot of measured and calculated temperatures, according to two finite-element models (FEM-1, FEM-2), against time.

to magnify any difference. When the measured temperature was plotted in this way for a number of locations in the rock, it was noticed that there is an abrupt decrease in slope in each curve around 100 - 140 days. In hydrology such a reduction in the slope of a semilog plot of drawn-down versus time indicates either the encounter of a constant head boundary or a general increase of transmissivity. When temperatures calculated using a finite-element model (FEM-1) with air temperature 18°C in the extensometer drift was plotted against the logarithm of time, no sudden change in slope could be discerned. This seemed to suggest that the sudden change of slope in the measured curve might indicate an increase in "effective thermal transmissivity," possibly due to fracture closure upon thermal expansion of the rock. To further test this hypothesis, the air temperature was measured in the extensometer drift and was found to be 10°C. Repeating the finite-element calculation using this air temperature produces the solid curve (FEM-2) in Fig. 4. This curve exhibits a sudden change in slope similar to the field data. Thus the shape of the observed temperature curve is more likely a consequence of boundary effect than of fracture closure. Note that the measured and calculated temperatures differ by no more than 2°C.

Conduction Through Heat Plug and Convection in Heater Hole

Two finite-element models have been used to estimate the effects of heat conduction through the vermiculite heat plug and free air convection in the upper portion of the heater hole. For one model (Model A) the heat plug and the air in the heater hole above the plug is considered to provide perfect insulation, while for the other (Model B) heat conduction through the heat plug is modeled using the thermal properties listed in Table 1 above and convective

boundary condition is applied to the portion of the heater hole above the heat plug. Measured air temperature profile, varying between 30°C just above the heat plug to 20°C at the top of the hole, was used in Model B. For 8 W/m^2-°C the maximum combined effect of convection in the hole and heat leakage through the plug at any thermocouple position in the rock is to lower the temperature at r = 0.4 m and z = 3 m by 1°C. For the first 10 days of the experiment Model B predicts a temperature up to 3°C higher than Model A at that same location. However, since the air temperature profile used in Model B was measured after the heater has been on for about 300 days, it is questionable whether this model is valid for the first 10 days. Effect of conduction through the vermiculite heat plug alone is less than 1°C anywhere in the rock.

Nonuniform Initial Rock Temperatures

Initial rock temperature, as recorded by thermocouples before the heater was turned on, decreases with increased depth below the heater drift approximately as follows: 14°C just beneath the floor, 11.4°C at a depth of 4.25 m below the floor, and 10°C at a depth of 9.25 m below the floor. This nonuniform temperature distribution is a consequence of the warm air in the drift.

To investigate the effect of this nonuniform initial temperature distribution, two separate finite-element runs were made. In the first run, actual variable initial temperatures were given; in the second a uniform initial temperature of 10°C was assigned to the rock throughout the model. The difference in temperatures for these two different cases diminishes with time. The maximum error due to the assumption of uniform initial temperature at any point is approximately equal to the difference between the actual value of the initial temperature and the value which has been fed to the model. After 50 days, the

error due to the assumption of uniform initial temperature at any thermocouple location is less than 1°C.

Incidentally, these calculations show that a nonuniform initial temperature distribution cannot be simply superimposed on the solution obtained from a model that assumes a uniform initial temperature. This is evident from the theory of partial differential equations, but has, unfortunately been neglected by some numerical analysts.

Temperature-Dependent Thermal Conductivity

Calculated radial variation of temperature in the midplane (z = 0) is shown on Fig. 5 for two different values of time, 10 and 100 days, for three cases, i.e., two different cases of constant k (thermal conductivity) and temperature-dependent k as given in Eq. (1). The temperature distribution obtained using temperature-dependent k lies between those predicted using the constant values, k = 3.2 W/m-°C and k = 3.7 W/m-°C. Thus the effect of material nonlinearity is not very significant. Maximum effects, occurring in the midplane, range between 2 to 5 degrees depending on time and radial distance from the heater. In the case of the 5 kW experiment, the effect of temperature-dependent thermal conductivity is slightly more significant. Material nonlinearity does not affect the shape of the vertical temperature profile.

Final Model

The final finite-element model for the present paper incorporates (a) the correct position of the heater, (b) convective boundary conditions in the heater and extensometer drifts as well as the heater hole, (c) conduction through the vermiculite heat plug, (d) nonuniform initial temperature distribution,

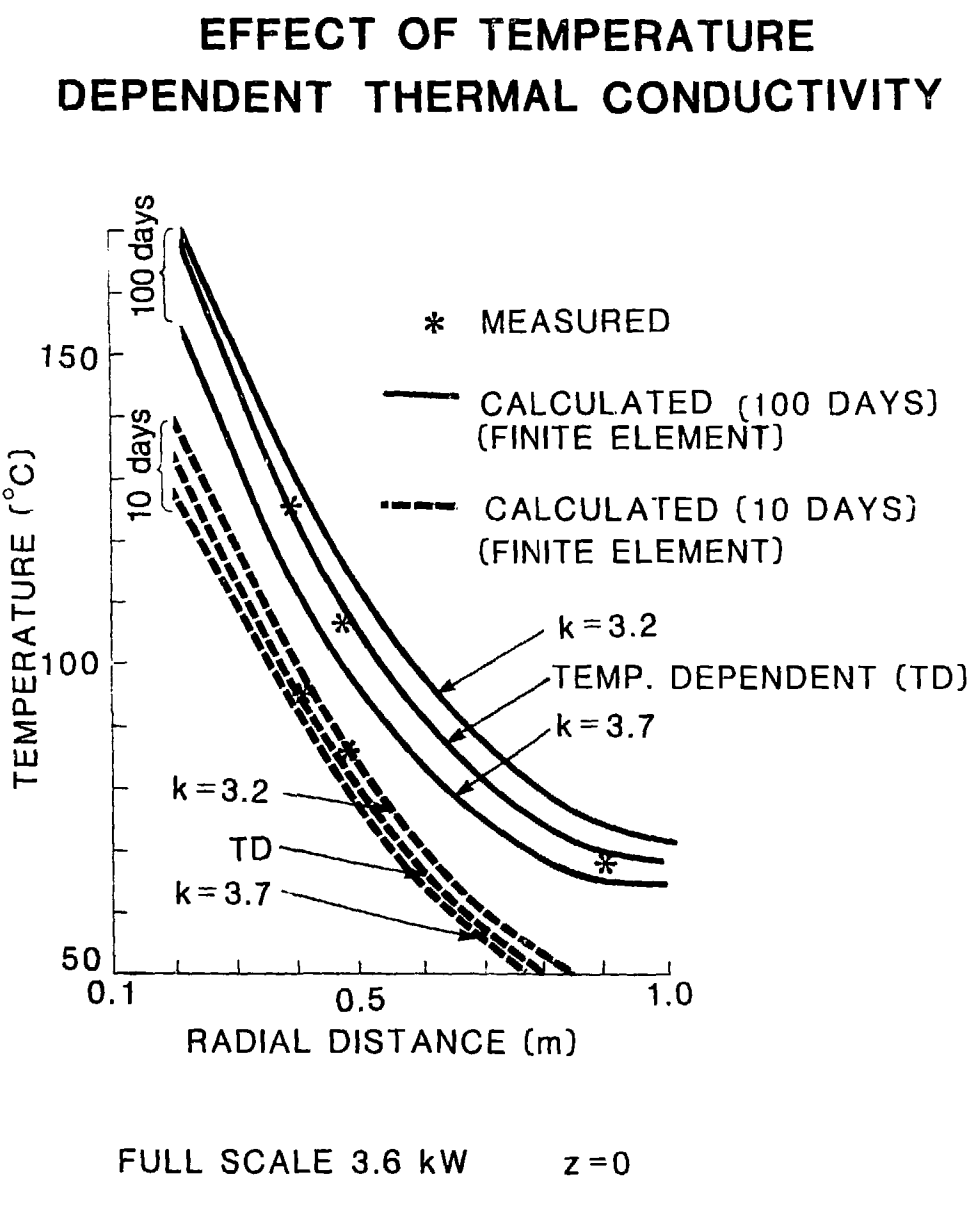

Fig. 5. Radial temperature distribution calculated using constant (3.2 or 3.7 W/m-°C) or temperature-dependent thermal conductivity, compared to field data.

and (e) temperature-dependent thermal conductivity as determined by small-specimen laboratory testing. Calculated and measured vertical temperature profiles at two different radial distances from the 3.6 kW heater are compared in Fig. 6. Note the steep thermal gradient around $z = \pm 1.5$ m. The modeled temperatures are also plotted against time in Fig. 3 (solid line). Both the predicted spatial and temporal variations of the rock temperatures are well in accord with field data. The largest discrepancies, ranging from 4°C to 8°C depending on radial distance from the heater, occur at $z = -1.5$ m.

DISCUSSION

Nearly all the essential features of the thermal field observed in the in situ heater experiment have been correctly duplicated by the finite-element model without invoking groundwater convection. The remaining discrepancies may be due to one or more of the following: (a) minor uncertainty (2 - 3 cm) in the position of the heater, (b) minor uncertainties in position (about 1 cm) and calibration of the thermocouples, (c) heat loss (less than 1% of total thermal power) through continuous operation of the air pump for the dewatering system in the heater hole, (d) influence of geological features such as the pegmatite dyke and several faults traversing the experiment area, and (e) slight differences between laboratory and in situ thermal properties including the possibility of higher effective thermal conductivity of the rock below the midplane of the heater.

Some indication of groundwater seepage through faults into the thermocouple holes below the midplane level is evident from a preliminary comparison of the spatial distribution of corroded thermocouples with fracture maps. Water seepage and steam formation may affect the temperature locally.

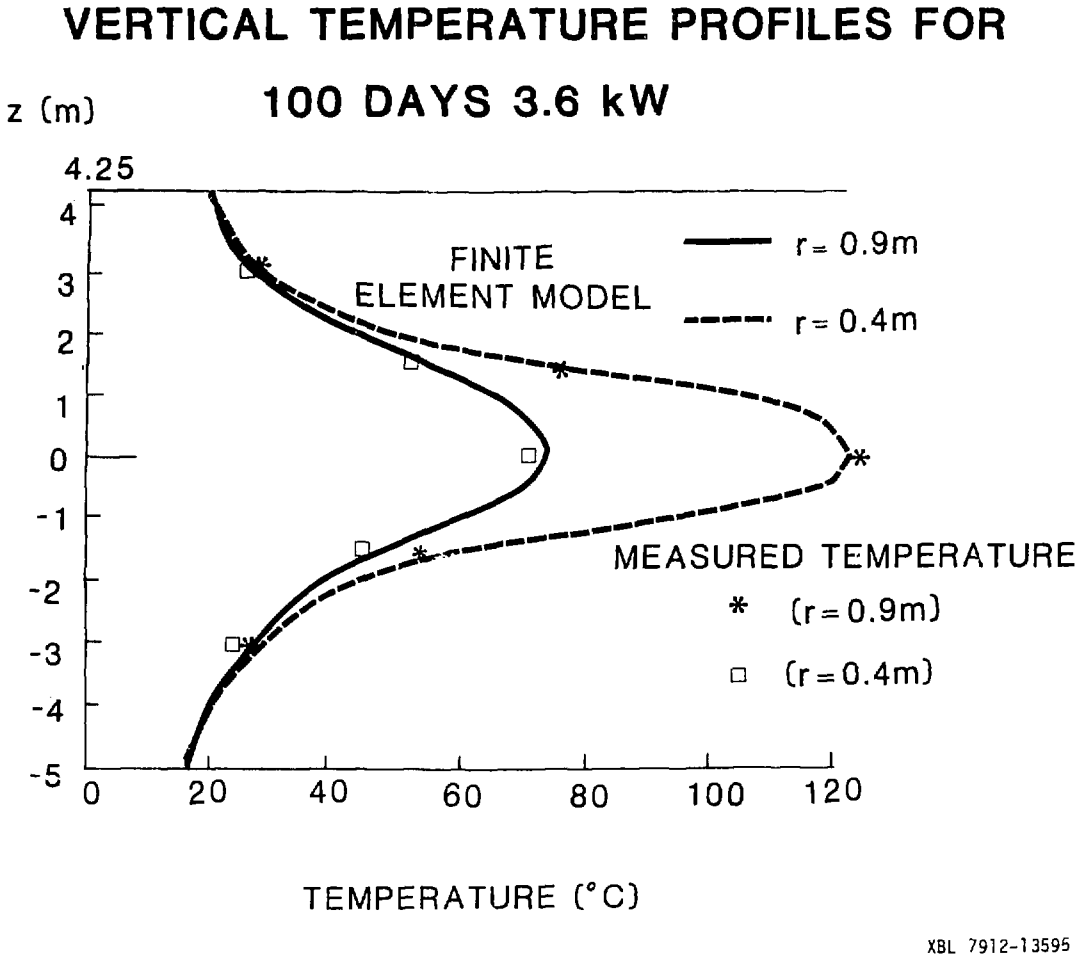

Fig. 6. Measured and modeled vertical temperature profiles at two different radii from heater.

Final resolution of the true cause of the minor discrepancies must await further exhaustive - and exhausting - data analysis.

CONCLUSION

Heat transfer in the heater experiment in Stripa granite is predominantly by conduction. Rock temperatures have been calculated quite accurately using a finite-element conduction model incorporating the proper initial and boundary conditions, temperature-dependent conductivity and other operating conditions. Groundwater convection does not contribute significantly to the heat transport. In spite of the time-varying thermal stresses and deformations in the rock mass, the thermal properties appear to remain essentially unaffected (except in the case of the 5 kW experiment, after borehole decrepitation). Minor local discrepancies still remain. These may perhaps be related to geological features.

ACKNOWLEDGEMENTS

This work was prepared under the auspices of the U. S. Department of Energy under contract W-7405-ENG-48. This project is managed by the Office of Nuclear Waste Isolation, Battelle, Columbus, Ohio. Numerous American and Swedish colleagues have participated in the field experiments. In addition to those whose names appear in the references, E. P. Binnall, H. Carlsson, A. DuBois and P. Nelson have contributed to the temperature measurements.

REFERENCES

1. Witherspoon, P. A. , and Degerman, O., "Swedish-American Cooperative Program on Radioactive Waste Storage in Mined Caverns - Program Summary" LBL-7049, SAC-01, Lawrence Berkeley Lab., Berkeley, CA. 94720, May, 1978.

2. Witherspoon, P. A., Cook, N. G. W., and Gale, J. E., "Geologic Storage of Radioactive Waste - Results from Field Investigations at Stripa, Sweden," Proc. of Waste Management '80, Univ. of Arizona, Tucson, Arizona, March, 1980.

3. Chan, T., Hood, M., and Board, M., "Rock Properties and Their Effect on Thermally-Induced Displacements and Stresses," presented at ASME 1980 Energy Technology Conference and Exhibition, New Orleans, February, 1980 submitted to ASME Journ. Energy Resources Tech.

4. Chan, T., Littlestone, N. and Wan, O., "Thermomechanical Modeling and Data Analysis for Heating Experiments at Stripa, Sweden." Proc. 21st U.S. Rock Mech. Symposium, Rolla, Mo., May 1980.

5. Kisner, R. A., et al., "Nuclear Waste Projections and Source-Term Data for FY 1977", Y/OWI/TM-34, Office of Waste Isolation, Oak Ridge, April, 1977.

6. Chan, T., Cook, N G. W., and Tsang, C. F., "Theoretical Temperature Fields for the Stripa Heater Project" LBL-7082, SAC-09, Lawrence Berkeley Lab., Berkeley, Ca. 94720, 1978.

7. Chan, T. and Remer, J. S., "Preliminary Thermal and Thermomechanical Modeling for Near Surface Test Facility Heater Experiment at Hanford," LBL-7069, Vol. 1, Lawrence Berkeley Lab., Berkeley, CA. 94720, 1978.

8. Combarnous, M. A., and Bories, S. A., "Hydrothermal connection in Saturated Porous Media," Advances in Hydroscience, Vol. 10, pp. 231-307, 1975.

9. Pratt, H. R., Schrauf, T. A., Bills, L. A., and Hustrulid, W. A., "Summary Report - Thermal and Mechanical Properties of Granite, Stripa, Sweden," TR 77-92, Terra Tek, Salt Lake City, Utah, 1977.

10. Chan, T., Hood, M., and Witherspoon, P. A., "Predicted and Measured Temperatures, Displacements and Stresses from the Stripa Heater Experiments", Proc. Rockstore 80. Special Session on Nuclear Waste Disposal, Stockholm, June, 1980. LBL-10358.

11. Jeffry, J. A., Chan, T., Cook, N. G. W., and Witherspoon, P. A., "Determination of In-Situ Thermal Properties of Stripa Granite from Temperature Measurements in the Full-Scale Heater Experiments." LBL-8423, SAC-24, Lawrence Berkeley Lab., Berkeley, CA., 1979.

12. Jaeger, J. C. and Cook, N. G. W. Fundamentals of Rock Mechanics, 2nd Ed., Wiley, New York, 1976, pp. 195-207.

13. Polivka, R. M. and Wilson, E. L., "Finite Element Analysis of Nonlinear Heat Transfer Problems." Report no. UC SESM 76-2, Dept. of Civil Eng., Univ. of Calif., Berkeley, Ca., June, 1976.

14. McAdams, W. H., Heat Transmission, 3rd Ed., McGraw Hill, Toronto, 1954.

15. Witherspoon, P. A. et al., "Large-Scale Permeability Measurements in Fractured Crystalline Rock", presented at the Intern. Geol. Congress, Paris, July, 1980.

16. Lundstrom, L., and Stille, H., "Large Scale Permeability Test of the Granite in the Stripa Mine and Thermal Conductivity Test," Report LBL-7049, Lawrence Berkeley Lab., Univ. of Calif., Berkeley, Ca., 1978.

APPENDIX A. HEAT TRANSFER BY CONDUCTION AND NATURAL CONVECTION IN THE GRANITE ROCK MASS AT STRIPA.

If, to a first approximation, the granite rock mass is treated as a saturated porous medium, then the ratio of heat transfer of the groundwater by natural convection to heat transfer through the saturated granite by conduction is given qualitatively [8] by the dimensionless Rayleigh number,

$$Ra = \frac{g k^{in} \rho_f^2 \alpha_f c_f \ell \Delta T}{\mu_f k} \qquad (2)$$

where all the quantities with subscript "f" refer to water properties at the reference temperature.

From in situ hydrology tests at the Stripa site [15,16], the intrinsic permeability, k^{in}, of the granite rock mass has been found to lie in the range 10^{-18} to 10^{-16} m^2. Using the higher value of permeability, along with characteristic length, ℓ = 5 m, temperature difference, ΔT = 200°C, thermal conductivity of the rock mass, k = 3.2 W/m-°C, and standard handbook values for water properties at atmospheric pressure, Eq. (2) yields the Rayleigh number given in Table 2 for three assumed values of the reference temperature. The very low Rayleigh number clearly shows that heat transfer for the heater experiments is primarily by conduction, except perhaps for local perturbations near a major fracture with a much higher permeability than the mean rock mass.

Note that the Rayleigh number is directly proportional to ℓ, Eq. (2). For a repository rock with a characteristic length of 1 km, convective heat transfer may become important for an effective permeability of 10^{-15} m^2 or higher.

Table 2. Properties of Water and Raleigh Number for Various Values of Reference Temperature

T (°C)	ρ_f (kg/m^3)	α_f (m^3/m^3-°C)	c_f (J/kg-°C)	μ_f (kg/ms)	Rayleigh number
10	999.7	1.00×10^{-4}	4.19×10^{3}	1.31×10^{-3}	9.8×10^{-5}
50	988.1	5.06×10^{-4}	4.18×10^{3}	5.48×10^{-4}	1.16×10^{-3}
100	958.4	7.30×10^{-4}	1.37×10^{2}	2.84×10^{-4}	9.8×10^{-5}

APPENDIX B. CLOSED-FORM INTEGRAL SOLUTIONS FOR LINEAR HEAT CONDUCTION.

For linear heat conduction in a homogeneous, isotropic continuum, closed form integral solutions for the temperature rise caused by a distributed, time-varying heat source can be derived using standard Green's function technique. Basically, the solution for an instantaneous point source is convolved with the source function in space and time. The solution for an arbitrarily time-varying heat source in the form of a finite-length line, a finite-length, finite-radius cylinder, and a finite-radius disc has been shown to be [6,7]:

$$\Delta T(r,z,t) = \frac{1}{8\pi k}\int_0^t Q_\ell(t-\mu)\left[\operatorname{erf}\left\{\frac{z+b}{2(\kappa\mu)^{1/2}}\right\} - \operatorname{erf}\left\{\frac{z-b}{2(\kappa\mu)^{1/2}}\right\}\right]\frac{1}{\mu}\exp\left(\frac{-r^2}{4\kappa\mu}\right)d\mu \tag{3}$$

for a line source,

$$\Delta T(r,z,t) = \frac{1}{4k}\int_0^t \frac{Q_c(t-\mu)}{\mu}\left[\operatorname{erf}\left\{\frac{z+b}{2(\kappa\mu)^{1/2}}\right\} - \operatorname{erf}\left\{\frac{z-b}{2(\kappa\mu)^{1/2}}\right\}\right] \int_0^a \exp\left\{-\frac{(r^2+r'^2)}{4\kappa\mu}\right\} I_0\left(\frac{rr'}{2\kappa\mu}\right) r'dr'd\mu \tag{4}$$

for a cylindrical source, and

$$\Delta T(r,z,t) = \frac{1}{4k(\pi\kappa)^{1/2}}\int_0^t \frac{Q_d(t-\mu)}{\mu^{3/2}}\int_0^a \exp\left[-\frac{r'^2+r^2+(z-z')^2}{4\kappa\mu}\right] I_0\left(\frac{rr'}{2\kappa\mu}\right) r'dr'd\mu \tag{5}$$

for a disc source.

FIGURE CAPTIONS

Fig. 1. Geometry of the 3.6 kW heater experiment, vertical section.

Fig. 2. Horizontal section through midplane of the 3.6 kW heater (at center) showing calculated isotherms (closed-form solution) together with measured temperatures at various thermocouple locations (asterisk) after 100 days.

Fig. 3. Measured and calculated temperatures as a function of time at radial distance 0.4m from the axis of the 3.6 kW heater and at various elevations.

Fig. 4. Semilog plot of measured and calculated temperatures, according to two finite-element models (FEM-1, FEM-2), against time.

Fig. 5. Radial temperature distribution calculated using constant (3.2 or 3.7 W/m-°C) or temperature-dependent thermal conductivity, compared to field data.

Fig. 6. Measured and modeled vertical temperature profiles at two different radii from heater.